

## PAPER DETAILS

TITLE: Shear Capacity Prediction of Extremely-Loaded Box Culvert on Elastic Soil Using Artificial Neural Network

AUTHORS: Yesim Tuskan,Dilay Yildirim Uncu

PAGES: 1103-1114

ORIGINAL PDF URL: <https://dergipark.org.tr/tr/download/article-file/3076311>

## Shear Capacity Prediction of Extremely-Loaded Box Culvert on Elastic Soil Using Artificial Neural Network

Yesim Tuskan<sup>\*</sup> , Dilay Yıldırım Uncu 

Manisa Celal Bayar University, Faculty of Engineering and Natural sciences, Department of Civil Engineering, Manisa, Türkiye, [yesim.tuskan@cbu.edu.tr](mailto:yesim.tuskan@cbu.edu.tr), [dilay.yildirim@cbu.edu.tr](mailto:dilay.yildirim@cbu.edu.tr)

<sup>\*</sup>Corresponding Author

### ARTICLE INFO

### ABSTRACT

#### Keywords:

Box culvert  
Beam on elastic foundation  
Traffic load  
Artificial neural network  
Winkler method



#### Article History:

Received: 11.04.2023

Accepted: 12.10.2024

Online Available: 23.10.2024

A box culvert, buried at shallow depths beneath roadways, may experience deflections caused by the dynamic impact of traffic loading and the vertical pressure exerted by the soil fill. A computational model commonly employed used to various engineering issues, including those in geotechnical applications, is the beam-on-elastic-foundation model. In this context, the Moment Distribution Method (MDM) must be applied to account for the elastic foundation. To achieve this, the internal forces acting on the ends of both exterior and interior walls are transferred to the beam-like bottom slab of the culvert, which rests on an elastic soil bed. Subsequently, the secondary internal forces are determined by refining the structural parameters, taking into account the characteristics of the elastic soil bed. This study presents the development and application of an Artificial Neural Network (ANN) model to predict the shear capacity of box culverts on elastic soil under traffic loading conditions. The proposed model is trained and validated using a comprehensive database of beam on elastic foundation solutions. The input parameters include the geometrical and mechanical properties of the culvert and the soil, as well as the loading conditions. The results of the ANN model show  $R^2$  values of 0.9633 and 0.9581 for the training and testing sets, respectively, indicating the model's excellent accuracy. These findings suggest that the ANN model can reliably predict the shear capacity of culverts.

## 1. Introduction

Box culvert installation is a commonly used methods on roadways to provide drainage across roads. According to the literature, there are various procedures for installing reinforced concrete box culverts. Embankment culverts are often the focus of initial finite element analyses and are typically characterized by their installation process. These culverts are usually positioned on pre-existing or constructed soil and then covered with backfill material [1]. A box culvert buried at shallow depths beneath roadways can experience deflections due to the dynamic impact of traffic loading and the vertical pressure exerted by the soil fill. The model, configuration, and magnitude of the traffic load

affect the culvert's response. Vertical soil stress increment, horizontal soil pressure, the culvert's self-weight, and wheel load are the major forces encountered in a culvert.

Yankelevsky [2] examined the behavior of a rigid box culvert when buried in a non-linear medium, exploring various factors. The research focuses on design aspects such as compressibility, stiffness, settlement, displacement due to trench wall slope, and depth-related stress variations. Kim and Yoo [3] indicated that sloping soils excavated for trench installation maintain higher resulting pressure than those with vertical walls. Beaver et al. [4] utilized a quantitative method to evaluate the structural and hydraulic performance of over 47,000 culverts installed

and managed by the Utah Department of Transportation. Their culvert inspections primarily included metal, concrete, and plastic culverts up to five feet in diameter, with numeric performance ratings determined. Pimentel et al. [5] investigated the pressure distribution on the top slab of culverts and observed a significant reduction due to soil-structure interaction. Bennett et al. [6] concluded that the geometry of the structure affected the pressure on the culvert under a high embankment. Abolmaali and Garg [7] conducted an assessment on the shear capacity of precast reinforced concrete box culverts.

The study involved subjecting six full-scale 2.4 m (8 ft) span box culverts to failure under the AASHTO HS-20 wheel load. Each culvert underwent incremental loading until failure, with crack initiation and propagation meticulously identified and recorded at each load stage. In some specimens, the absence of top slab compression distribution steel during fabrication was noted; however, experimental evidence suggested that this factor had a insignificant impact on the culvert's performance.

3D numerical analyses of culverts conducted by Petersen [8] showed that the pavement spread the load and shielded the culvert. Wood et al. [9] compared measured demands with predicted values using analytical tools during load testing of box culverts and found that pavement stiffness plays an important role in reducing live loads on the culvert's roof. The effect of the wheel loads from traffic is a significant factor in the performance of culverts installed at shallow depths. Additionally, the live load carrying rating must be determined to assess the culvert's load capacity. Three major factors influence load capacity: culvert load capacity, dead load demand, and live load demand for moment and shear [10]. Wood et al. [11] studied both a 2D direct-stiffness structural-frame model and a 2D linear-elastic finite element soil-structure interaction model.

The culvert structure is designed as a rigid frame using the Moment Distribution Method (MDM), a well-known method to determine the final distributed moments based on the relative stiffness of the slab and vertical walls [12]. MDM

calculations, which involve successive cycles of computation, can be stopped after several iterations, providing a very accurate approximate analysis. In this method, each element of rigid box-type culvert, such as the top and bottom slabs, and the interior and exterior walls is treated as a beam-like element, with the corners of the box clamped.

The MDM requires the fixed-end moments at the top slab of the culvert from the uniform surcharge load, referred to as critical vertical pressure, the fixed-end moments at the bottom slab from uniform vertical earth pressure, and the fixed-end moments on the exterior walls from lateral earth pressure due to cohesionless soil. These moments are then distributed and carried over accordingly [13].

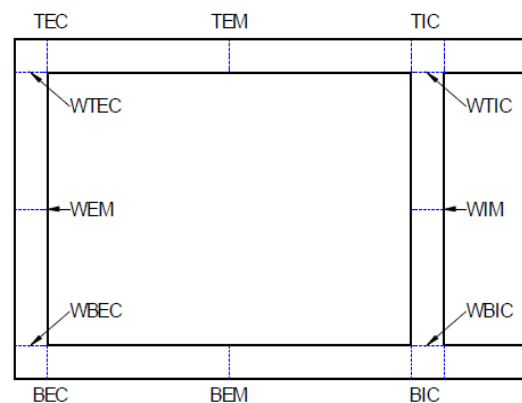


**Figure 1.** Internal forces at the corners and mid-spans of each elements of culvert

The primary internal forces related to the wall top interior corner (WTIC), top exterior corner (TEC), top interior corner (TIC), top exterior mid-span (TEM), and wall top exterior corner (WTEC) are calculated by considering the fixed-end moments and external loads (Figure 1). Finally, the diagrams for normal forces (kN), shear forces (kN) and moments (kN.m) are determined at the corners and mid-spans of each elements of the culvert.

## 2. Shear Capacity Prediction of a Box Culvert Under Critical Live Load as per Beams on Elastic Foundation Approach Using Artificial Neural Network

The computational model of a beam on an elastic foundation is frequently used to solve various engineering problems, particularly in geotechnical applications. In this case, the MDM

results need to be adapted to the elastic foundation. For this aim, the internal forces at the ends of the exterior and interior walls are applied to the beam-like bottom slab of the culvert resting on an elastic soil bed. The secondary internal forces are calculated by refining the structural factors, taking into account the elastic soil bed.

### 2.1. Vertical pressure calculation by Boussinesq Method on top slab of box culvert subjected to traffic load

Boussinesq [14] solved the problem of tension arising from a single load on the surface in a linear, elastic, homogeneous, isotropic, and semi-infinite medium. According to this solution, the vertical stress at any depth below the earth's surface due to a single surface load is expressed follows:

$$\sigma_z = \frac{3}{2\pi} \frac{1}{[1+(r/z)^2]^{5/2}} \cdot \frac{P}{z^2} \quad (1)$$

where P is the point wheel load (Truck geometry: H<sub>30</sub>-S<sub>24</sub>, W<sub>truck</sub>=300 kN, wheel loads; P<sub>front</sub>=3 tons, P<sub>rear</sub>=P<sub>middle</sub>=12 tons, s=75 cm, t=34 cm), r is radial distance from point wheel load and z: soil depth above the box culvert.

For practical purposes, it can be assumed that the stress approaches zero at a finite depth. A grid system was established on the platform, and the stress at the considered depth for each grid point was determined by applying the superposition of wheel loads from trucks travelling in the two different directional lanes on the same platform roadway. This was done by integrating the equation for a line load over a uniformly loaded rectangular area. The following equation provides the desired stress superposition [15].

$$\begin{aligned} \sigma_z &= q_0 \left( \frac{1}{4\pi} \right) \left[ \frac{2mn\sqrt{(m^2+n^2+1)}}{(m^2+n^2+1+m^2n^2)} \frac{(m^2+n^2+2)}{(m^2+n^2+1)} \right. \\ &\quad \left. + \arctan \frac{2mn\sqrt{(m^2+n^2+1)}}{(m^2+n^2+1-m^2n^2)} \right] \quad (2) \end{aligned}$$

Where  $\sigma_z$ ; superposition of vertical pressure subjected to each wheel load at the considered depth z,  $q_0$ ; the contact stress at the surface {P/(s.t)},  $m=x/z$ ,  $n=y/z$ , x-y; length and width of

the uniformly loaded area and z; depth from surface to point where stress increase is desired [16].

### 2.2. Lateral earth pressure acting on side walls of box culvert

According to Coulomb's theory, the active coefficient factor of active lateral earth pressure in cohesionless soil were calculated by using Eq 3a and 3b:

$$K_A = \frac{\sin^2(\beta+\phi)}{\sin^2\beta \sin(\beta-\delta) \left[ 1 + \sqrt{\frac{\sin(\phi+\delta) \sin(\phi-\alpha)}{\sin(\beta-\delta) \sin(\alpha+\beta)}} \right]^2} \quad (3a)$$

$$\sigma_h = K_A \gamma_s (z + h_{eq}) \quad (3b)$$

Then the increase in horizontal pressure due to live load was obtained from Eq 4:

$$\Delta P = K_A h \gamma_s h_{eq} \quad \{\Delta P = \sigma_z\} \quad (4)$$

where  $K_A$ ; active lateral earth pressure coefficient,  $\delta$  is angle of internal friction of soil,  $\phi$ ; batter angle of wall;  $\beta$  is angle of friction between the wall and the cushion,  $\alpha$ ; slope of the cushion top surface,  $\gamma_s$ ; unit weight of soil, z; depth below the surface of earth at pressure surface ( $h_{eq}$  should be added to the original soil depth z in case of surcharge loads).  $\sigma_z$ ; vertical pressure due to surcharge load,  $\Delta P$ ; constant horizontal earth pressure due to live load surcharge and  $h_{eq}$ ; equivalent height of soil for traffic load.

### 2.3 Elastic soil under box culvert

The Winkler method [17] assumes that the reaction forces at each point of the foundation under external loads are proportional to the deflection of the beam at that point, following Hooke's law (Figure 2).

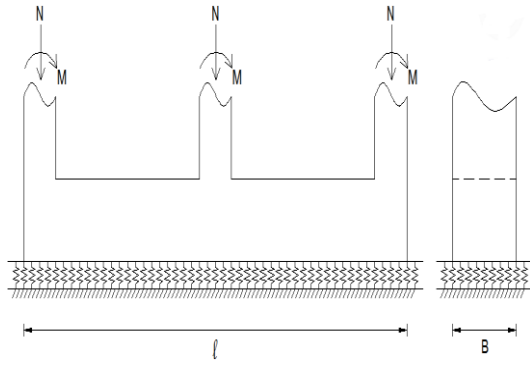


**Figure 2.** Beam on elastic foundation

The elasticity of the foundation, characterized by Winkler's constant,  $K$  which includes the effect of the width of the beam, the force called the modulus of the foundation  $K_o$ .  $\lambda$  are described by the following equations 5 and 6 [18]:

$$K = K_o \cdot B \quad (5)$$

$$\lambda = \sqrt[4]{\frac{K}{4EI}} \quad (6)$$

In this study, internal forces such as moments and shear forces at the lower ends of the baffle and side walls are calculated by using the Moment Distribution Method (MDM) and are subsequently applied to the unit width of the lower slab over elastic soil bed, in accordance with the following equations.

Moments and shear forces equations of unit width beam-like slab on elastic foundation for concentrated load can be expressed as:

$$M_{(x)} = \frac{1}{2\lambda} \beta_{MP}^{(x)} \frac{1}{(\sinh^2 \lambda l - \sin^2 \lambda l)} \{2 \sinh \lambda x \cdot \sin \lambda x (\sinh \lambda l \cdot \cos \lambda a \cdot \cosh \lambda b - \sin \lambda l \cdot \cosh \lambda a \cdot \cos \lambda b) + (\cosh \lambda x \cdot \sin \lambda x - \sinh \lambda x \cdot \cos \lambda x) \cdot [\sinh \lambda l (\sin \lambda a \cdot \cosh \lambda b - \cos \lambda a \cdot \sinh \lambda b) + \sin \lambda l (\sinh \lambda a \cdot \cosh \lambda b - \cosh \lambda a \cdot \sin \lambda b)]\} \quad (7)$$

$$Q_{(x)} = P \beta_{QP}^{(x)} \frac{1}{\sinh^2 \lambda l - \sin^2 \lambda l} \{(\cosh \lambda x \cdot \sin \lambda x + \sinh \lambda x \cdot \cos \lambda x) (\sinh \lambda l \cdot \cos \lambda a \cdot \cosh \lambda b - \sin \lambda l \cdot \cosh \lambda a \cdot \cos \lambda b) + \sinh \lambda x \cdot \sin \lambda x [\sinh \lambda l (\sin \lambda a \cdot \cosh \lambda b - \cos \lambda a \cdot \sinh \lambda b) + \sin \lambda l (\sinh \lambda a \cdot \cosh \lambda b - \cosh \lambda a \cdot \sin \lambda b)]\} \quad (8)$$

Moments and shear forces equations of unit width beam-like slab on elastic foundation for concentrated moment can be expressed as:

$$M_{(x)M} = -M \delta_{MM}^{(x)} = -M \frac{1}{(\sinh^2 \lambda l - \sin^2 \lambda l)} \{ \sinh \lambda x \cdot \sin \lambda x [\sinh \lambda l (\cosh \lambda b \cdot \sin \lambda a + \sinh \lambda b \cdot \cos \lambda a) + \sinh \lambda l (\sinh \lambda a \cdot \cos \lambda b + \cosh \lambda a \cdot \sin \lambda b)] - [(\cosh \lambda x \cdot \sin \lambda x - \sinh \lambda x \cdot \cos \lambda x) (\sin \lambda l \cdot \cos \lambda b \cdot \cosh \lambda a + \sin \lambda l \cdot \cosh \lambda b \cdot \cos \lambda a)] \} \quad (9)$$

$$Q_{(x)M} = -\lambda M \beta_{QM}^{(x)} = \frac{M}{e} \lambda l \frac{1}{(\sinh^2 \lambda l - \sin^2 \lambda l)} \{(\cosh \lambda x \cdot \sin \lambda x + \sinh \lambda x \cdot \cos \lambda x) [\sinh \lambda l (\cosh \lambda b \cdot \sin \lambda a + \sinh \lambda b \cdot \cos \lambda a) + \sin \lambda l (\sinh \lambda a \cdot \cos \lambda b + \cosh \lambda a \cdot \sin \lambda b)] - 2 \sinh \lambda x \cdot \sin \lambda x (\sin \lambda l \cdot \cos \lambda b \cdot \cosh \lambda a + \sinh \lambda l \cdot \cos \lambda b \cdot \cos \lambda a)\} \quad (10)$$

Concentrated load and concentrated moment in accordance with integral of a beam on an elastic foundation are described by the following equations:

$$M_{(x)M} = -M \delta_{MM}^{(x)} \quad (11)$$

$$Q_{(x)M} = -\lambda \beta_{QM}^{(x)} = -\frac{\lambda l}{I} M \beta_{QM}^{(x)} = -M \delta_{QM}^{(x)} \quad (12)$$

$$M_{(x)} = PL \frac{1}{\lambda l} \beta_{MP}^{(x)} = Pl \delta_{MP}^{(x)} \quad (13)$$

$$Q_{(x)} = P \beta_{QP}^{(x)} = P \delta_{QP}^{(x)} \quad (14)$$

### 3. Case Study

The observed rigid two-cell box-shaped culvert is aligned perpendicularly to the two-lane highway. The cushion material lies under a 250 mm asphalt concrete pavement.

A parametric study is conducted to assess the effect of the soil parameters, burial depth, box culvert dimensions (mm), and traffic load (kN) (Figure 3).

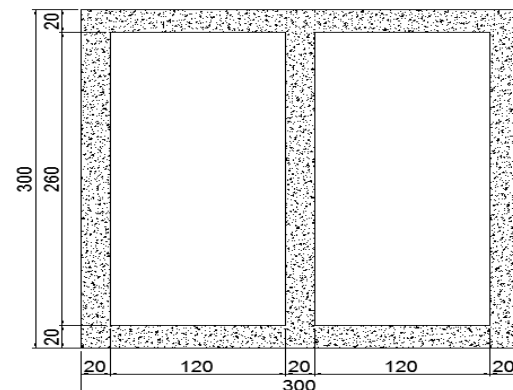


**Figure 3.** The cross-section of the box culvert

The culvert extends under the sloping embankment area on each side of the road. The embankment has a dry unit weight of about  $18 \text{ kN/m}^3$ , a saturated unit weight of  $21 \text{ kN/m}^3$  and shear strength parameter of  $\phi=40^\circ$ ,  $c=5 \text{ kN/m}^2$ , with  $K_0=50000$ ,  $E=3 \times 10^7 \text{ kN/m}^2$ , and  $I=6.6 \times 10^{-4} \text{ m}^4$ . The wheel spacing of design vehicle (Figure 4) was 1.8 m. (6 ft.) according to H<sub>30</sub>-S<sub>24</sub> truck axle loads. Since truck types with long rear axle distances are generally more common, the distance between the rear axles was chosen to be long.

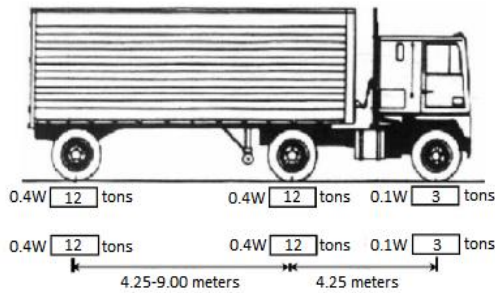


Figure 4. H<sub>30</sub>-S<sub>24</sub> truck axle loads

### 3.1. Critical vertical pressure subjected to wheel load and uniform surcharge load

Although the front axial load is much lower than those of rear axles, its contribution is included in calculating the superposition of all wheel loads of two design trucks by Boussinesq's [14] equation.

In this study, a 300 kN-load per wheel is considered for two design trucks with three axles each, traveling in opposing directions. It was determined that the second case has the highest vertical pressure. Therefore, the maximum pressure over the culvert is calculated as  $2.27 \text{ kN/m}^2$  and is taken as uniform surcharge load in design (Figure 5).

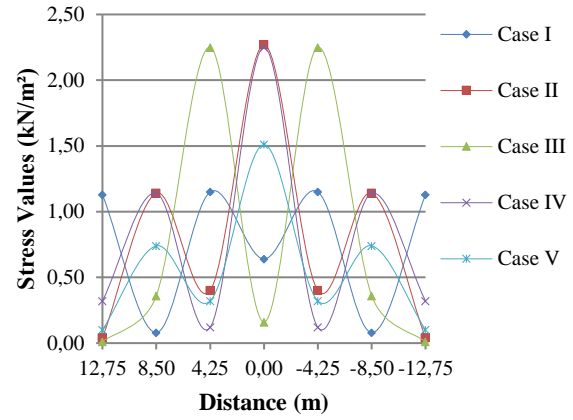


Figure 5. Stress distributions on the axis according to the loading conditions

To determine the extreme loading conditions for tridem-trucks traveling simultaneously in two lanes, five possible passing scenarios are considered as Case I: The front axles overlapped at one line, Case II: The middle axles overlapped at one line, Case III: The mid-spans of trailer lengths overlapped at one line, Case IV: The rear axles overlapped at one line and Case V: The cross axles overlapping (Figure 6).

The critical vertical pressure can be calculated using Eq 2. The vertical pressure combinations from the wheel loads were evaluated for the five possible passing conditions of trucks (Figure 6). The different distributions of wheel load recommended by proposed scenarios caused the vertical pressure concentration affecting the top slab shear resistance of the culvert. For the highest wheel load concentration, the stress was greatest between the edge and the center, as shown in Figure 6.

An analytical solution to the beam problem on an elastic foundation is investigated to obtain the improved final bending moments and shear forces from the secondary structural analysis, as presented in Figure 7.



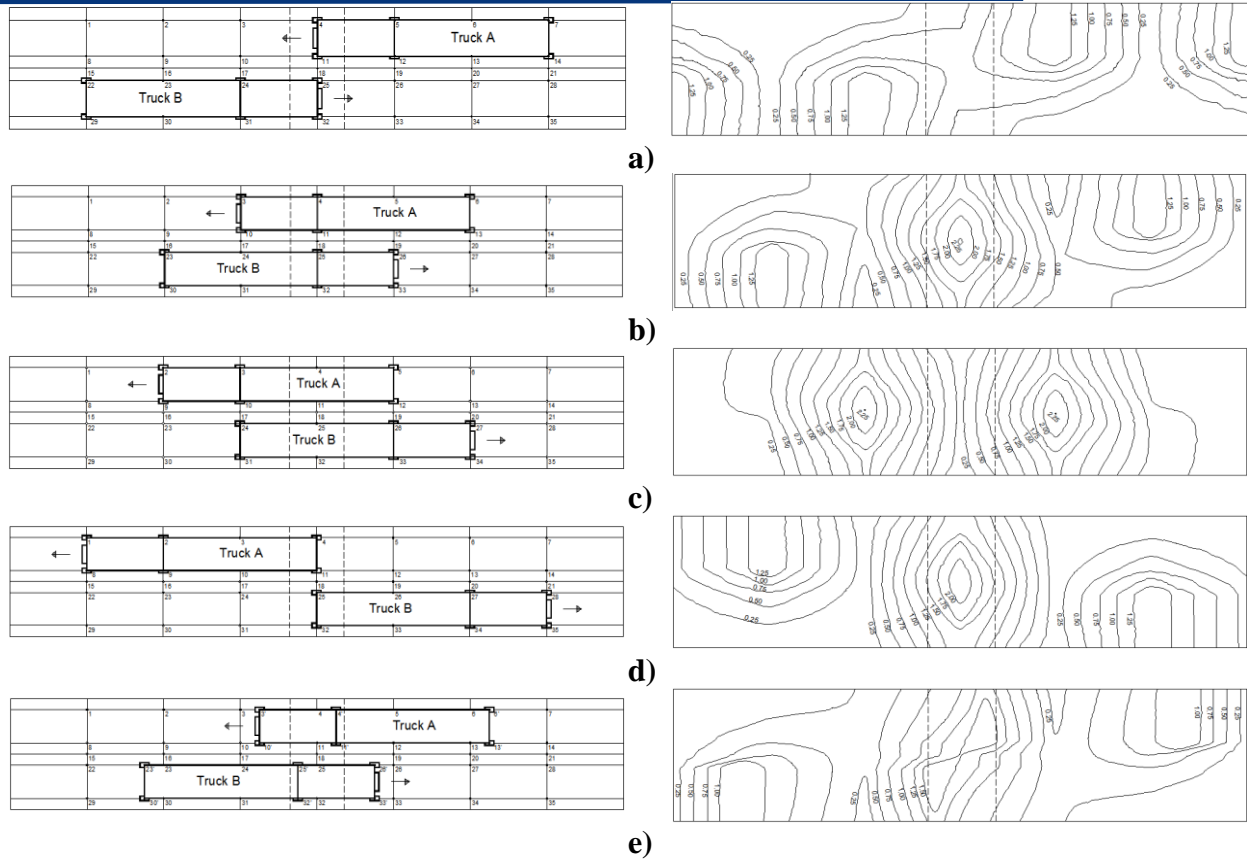


**Figure 6** The situations of the truck passing positions and relevant stress distribution: a) Case I: The front axles overlapped at one line, b) Case II: The middle axles overlapped at one line, c) Case III: The mid-spans of trailer lengths overlapped at one line, d) Case IV: The rear axles overlapped at one line and e) Case V: The cross axles overlapping

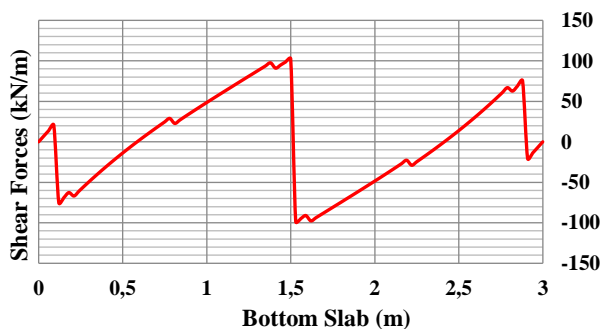
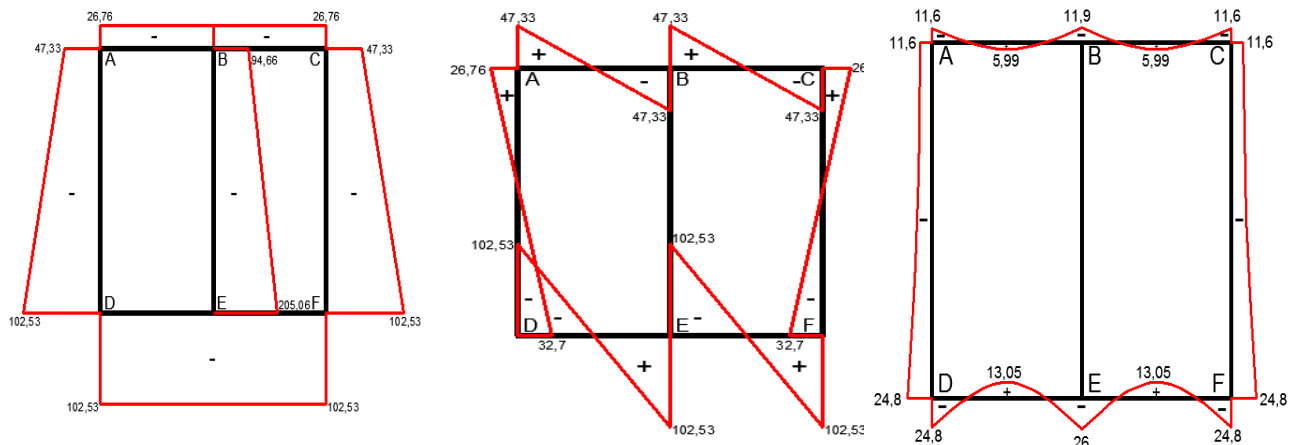


**Figure 7.** Shear diagram of box culvert as beam on elastic foundation

The diagrams for normal forces (kN), shear forces (kN) and moments (kN.m) are presented in Figure 8 (a, b, c) respectively.

The overall results for the beam on elastic foundation analysis, including the input parameters such as the geometrical and mechanical properties of the culvert and soil, as well as the loading conditions, along with the output parameter of the shear capacity of the top slab, are summarized in Table 1.



(a) (b) (c)  
**Figure 8. (a) The normal forces (kN), (b) shear forces (kN) and (c) moments (kN.m)**

**Table 1. Results of shear capacity on box culvert used for training and testing set**

	Data Number	Depth of cushion (hr) (mm)	Height of culvert (H) (mm)	Width of culvert (B) (mm)	Thickness of top slab ( $t_{ts}$ ) (mm)	Soil friction angle ( $\phi$ )	Soil unit weight ( $\gamma$ )	Wheel load (WL) (kN)	FS <sub>shear</sub>
Training Set	1	700	1100	1100	110	30	18	30	1.08
	2	750	1100	1100	110	30	18	30	1.17
	3	800	1100	1100	110	30	18	30	1.259
	4	850	1100	1100	110	30	18	30	1.345
	5	900	1100	1100	110	30	18	30	1.428
	6	950	1100	1100	110	30	18	30	1.507
	7	1000	1100	1100	110	30	18	30	1.582
	8	700	1200	1200	120	30	18	30	1.115
	9	750	1200	1200	120	30	18	30	1.208
	10	800	1200	1200	120	30	18	30	1.299
Testing Set	112	950	1100	1100	110	40	19	40	1.447
	113	800	2000	2000	200	40	19	40	1.315
	114	850	2000	2000	200	40	19	40	1.404
	115	900	2000	2000	200	40	19	40	1.489
	116	950	2000	2000	200	40	19	40	1.57
	117	1000	2000	2000	200	40	19	40	1.645
	118	700	3000	3000	300	40	19	40	1.125
	119	750	3000	3000	300	30	19	40	1.218
	120	800	2000	2000	200	30	19	40	1.315
	121	850	2000	2000	200	30	19	40	1.404
	122	900	2000	2000	200	30	19	40	1.489
	140	1000	3000	3000	300	40	19	40	1.655

#### 4. Artificial Neural Networks

Artificial Neural Networks (ANNs) are sophisticated computational models inspired by the behavior of the human brain and nervous system. Emerging artificial intelligence techniques have shown great sensitivity in predicting actual values without lengthy observational processes [19,20].

At this point, artificial neural networks (ANNs) have clear advantages in addressing complex non-linear problems in the field of civil the optimum weight combination of these neurons of feed-forward neural networks with various combinations of network and training parameters, including number of hidden layers is the back-propagation (BP) algorithm [27] Feed-

engineering [21,22]. These complex relationships are estimated by artificial neural networks with high accuracy [23-26]. In this regard, ANNs offer several advantages over more conventional computing techniques. A typical ANN architecture is constitutes by layers including an input layer, one or more hidden layer(s) and an output layer. Each layer basically contains a number of neurons working as an independent processing element and densely interconnected with each other. The method most commonly used for finding

forward neural network is trained by a fastest BP algorithm called Levenberg-Marquardt [27] Levenberg-Marquardt was used to improve the speed and general performance of BP [27]. An activation function governs a summing process



by multiply inputs by its weights. Training process terminates its cycles with a minimal sum squared error.

ANNs have a natural property for storing experiential knowledge of data and making it available for use of the problem solving as an interconnected group of artificial neurons [27]. According to above mentioned definitions, an ANN is considered one of the most powerful techniques inspired by the human-brain information process in soft computation method [28].

The assignment of the ANN architecture is difficult task to obtain. Currently, there is no analytical way of defining the network structure as a function of the complexity of the problem to achieve the desired accuracy.

An optimal ANN architecture is considered as the one yielding the best performance in terms of error minimization, while retaining a simple and compact structure [27]. Specifying the network architecture and detecting the optimal values for the connection weights of a training algorithm constitutes two main issues concerning the implementation of the ANN. The architecture arranged in a sequence of layers, one for the input, one for hidden layer and one for the output was used for ANN model (Figure 9).

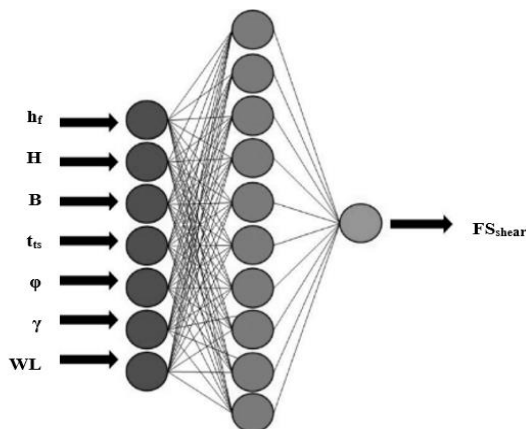


**Figure 9.** The ANN's architecture

Data from several scenarios were determined by utilizing an ANN architecture consisting of one input layer, one hidden layer, and one output layer. The data derived from the several shear capacity calculations have identified that, even by using one hidden layer, any complex function in a network can be solved [29]. Thus, one hidden

layer was selected in the ANN model using 10 hidden neurons provides the most accurate and minimum error.

Developing an optimum ANN architecture is a time-consuming operation because of the insufficient nonlinear relationship between input and output layers of the small structures [30]. However, a large structure provides a complex problem and requires a significant amount of time to train without well generalization. The literature shows that the number of neurons in the hidden layer ( $N_{hn}$ ) has a significant effect on the system's nonlinearity [31]. Thus,  $N_{hn}$  is the key factor for a proper mapping in which data flows between the input and output layers, resulting in good predicting using ANN.

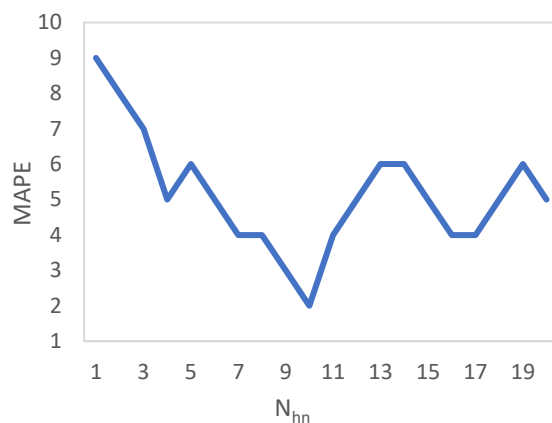


**Figure 10.** MAPE- $N_{hn}$  relation of the ANN architecture.

The prediction performance and the influence of the  $N_{hn}$  has been evaluated using mean absolute percentage error (MAPE). The minimum MAPE has been reached in the combination with  $N_{hm} = 10$ , showing the optimum architecture (Figure 10).

**Table 2.** Details of the parameters used for the ANN model

Data Type	Model Parameters	Minimum Value	Maximum Value	Mean Value
Input	Depth of cushion ( $h_f$ ) (mm)	700	1000	850
	Height of culvert (H) (mm)	1100	3000	1754.29
	Width of culvert (B) (mm)	1100	3000	1754.29

Thickness of top slab ( $t_{ts}$ ) (mm)	110	300	175.43	
Soil friction angle ( $\phi$ )	30	40	35	
Soil unit weight ( $\gamma$ )	18	19	18.50	
Wheel load (WL) (kN)	30	40	35	
Output	$FS_{\text{shear}}$	1.03	1.72	1.38

Subsequently, the data classification of the ANN model is based on the use of 80% of the data for training and 20% for testing, as suggested by Shahin et al. [32]. The network capacity is characterized by testing phase results emphasizing data generalization. In the model, LM algorithm is utilized to assemble the ANN model, while applying log sigmoid as the transfer function. The details of the parameters examined throughout the ANN analysis are dedicated in Table 2 for proposed scenarios.

## 5. Results and Discussion

Based on different scenarios of extreme loading of reinforced concrete culvert with different geometries and soil conditions, the ANN values modeled by multi-layer perception were shown in Figs. 11 and 12. An overall good agreement between ANN model and conventional results of beam on elastic foundation has been found.

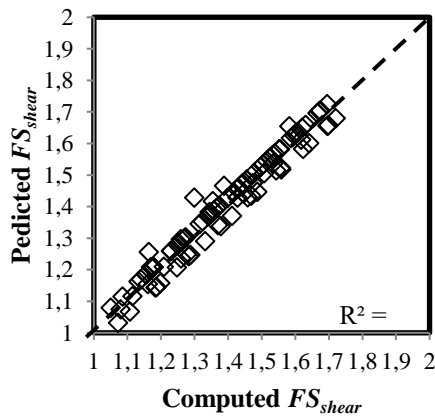


**Figure 11.** The comparison of the computed  $FS_{shear}$  of top slab values with the predicted  $FS_{shear}$  of top slab values from the ANN model for training samples

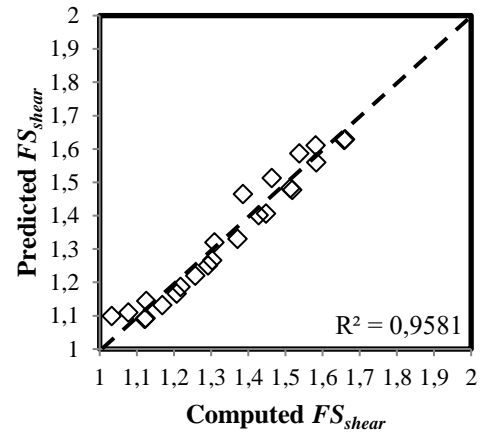


**Figure 12.** The comparison of the computed  $FS_{shear}$  of top slab values with the predicted  $FS_{shear}$  of top slab values from the ANN model for testing samples

Subsequently, the performance of the ANN was evaluated in Table 3 with four factors: coefficient of determination ( $R^2$ ), mean absolute error (MAE), variance accounted for (VAF) and mean square error (RMSE) to predict the accuracy of the proposed ANN model. The suitability of the model was verified with the ranges of performance indices.

**Table 3.** Performance indices ( $R^2$ , RMSE, MAE and VAF) of the ANN and model

Model	Data	$R^2$	RMS E	MAE	VAF
ANN	Trainin	96.3			95.2
	g set	3	0.82	0.43	8
	Testin	95.8			94.7
	g set	1	1.23	0.76	5

It is noted from the results of the ANN model has the  $R^2$  value of 0.9633 and 0.9581 for training and testing set, respectively indicating a perfect accuracy of the proposed model in this study.

## 6. Conclusion

In this study, the efficiency of the ANN model to predict the shear capacity of top slab ( $FS_{shear}$ ) has been investigated and compared. To achieve this, the  $FS_{shear}$  values were computed by changing the applied wheel load, soil friction angle, box culvert geometry and fill conditions from road level and utilized in the simulation of the ANN model. The input parameters used in the ANN model are five geotechnical parameters containing geometry component of box culvert ( $H$ ,  $B$ , and  $t_{ts}$ ), soil condition ( $\phi$  and  $\gamma_{soil}$ ) and

traffic condition (wheel load, WL) with depth of cushion ( $h_f$ ). The output parameter of the model is the computed shear capacity of top slab ( $FS_{\text{shear}}$ ) by using beam on elastic foundation approach.

It can be concluded that the ANN model developed in this study can be used for the estimation of the  $FS_{\text{shear}}$  value and so for the determination of the top slab shear capacity of extremely loaded reinforced concrete culvert on elastic soil.

In conclusion, the suitability of the model has been rigorously evaluated through comprehensive performance index evaluations, and the findings confirm the model's outstanding accuracy, demonstrating its potential as a reliable method for the chosen rear axle distance. However, for future research efforts, it would be appropriate to investigate comparative analyses with different axle distances using various soft-computing methodologies.

## Article Information Form

### *Funding*

The author(s) has no received any financial support for the research, authorship or publication of this study.

### *Authors' Contribution*

The authors contributed equally to the study.

### *The Declaration of Conflict of Interest/ Common Interest*

No conflict of interest or common interest has been declared by the authors.

### *The Declaration of Ethics Committee Approval*

This study does not require ethics committee permission or any special permission.

### *The Declaration of Research and Publication Ethics*

The authors of the paper declare that they comply with the scientific, ethical and quotation rules of SAUJS in all processes of the paper and that they do not make any falsification on the data collected. In addition, they declare that Sakarya University Journal of Science and its editorial

board have no responsibility for any ethical violations that may be encountered, and that this study has not been evaluated in any academic publication environment other than Sakarya University Journal of Science.

### *Copyright Statement*

Authors own the copyright of their work published in the journal and their work is published under the CC BY-NC 4.0 license.

## References

- [1] W. D. Lawson, T. A. Wood, C. D. Newhouse, P. W. Jayawickrama, "Evaluating Existing Culvert for Load Capacity Allowing for Soil Structure Interaction". Multidisciplinary Research in Transportation, 2010.
- [2] David Z. Yankelevsky., "Loads on Rigid Box Buried in Nonlinear Medium", Journal of Transportation Engineering, Vol. 115, No. 5, September, 1989. @asce, ISSN 0733-947X/89/0005-0461. Paper No. 23870.
- [3] K. Kim, C. Yoo, "Design Loading for Deeply Buried Box Culverts", Highway Research Center, Auburn University, 2002.
- [4] J. L. Beaver, T. J. McGrath, B. Leonard, "Condition Assessment of Utah Highway Culverts and Determination of Culvert Performance Measures", In Critical Transitions in Water and Environmental Resources Management, 2004, pp. 1-10.
- [5] M. Pimentel, P. Costa, C. Félix, J. Figueiras, "Behavior of reinforced concrete box culverts under high embankments", Journal of Structural Engineering, vol.135, no.4, pp.366-375, 2009.
- [6] R. M. Bennett, S. M. Wood, E. C. Drumm, N. R. Rainwater, "Vertical loads on concrete box culverts under high embankments", Journal of Bridge Engineering, vol. 10, no. 6, pp. 643-649, 2005.

- [7] A. Abolmaali, A. K. Garg, "Effect of Wheel live load on Shear Behaviour of Precast Reinforced Concrete Box Culverts." *Journal of Bridge Engineering*, Vol. 13, No.1, January 1, 2008, @ ASCE, ISSN 1084-0702/200/1-93-99.
- [8] D. L. Petersen, "Recommended design specifications for live load distribution to buried structures", *Transportation Research Board*, vol. 647, 2010.
- [9] T. A. Wood, W. D. Lawson, P. W., Jayawickrama, C. D. Newhouse, "Evaluation of production models for load rating reinforced concrete box culverts", *Journal of Bridge Engineering*, vol. 20, no.1, 04014057, 2015.
- [10] W. D. Lawson, T. A. Wood, C. D. Newhouse, P. W. Jayawickrama, "Evaluating existing culverts for load capacity allowing for soil structure interaction", *Texas DOT*, Austin, TX, 2010.
- [11] T. A. Wood, W. D. Lawson, P. W. Jayawickrama, "Newhouse, Evaluation of Production Models for Load Rating Reinforced Concrete Box Culverts", *The Journal of Bridge Engineering*, pp.1-12, 2014.
- [12] N. Kolate, M. Mathew, S. Mali, "Analysis and Design of RCC Box Culvert", *International Journal of Scientific & Engineering Research*, 5(12), 2014.
- [13] W. F. Chen, J. Y. Liew, "The Civil Engineering Handbook", Second Edition, *National University of Singapore*, CRC Press. 2003.
- [14] J. Boussinesq, "Application des potentiels à l'étude de l'équilibre et du mouvement des solides élastiques: Principalement au calcul des deformations et des pressions que produisent, dans ces solides, des efforts quelconques exercés sur une petite partie de leur surface ou de leur intérieur; mémoire suivi de notes étendues sur divers points de physique mathématique et d'analyse", *Gauthier-Villars*, 1885.
- [15] R. A. Cook, D. Bloomquist, "Report on Evaluation of Precast Box Culvert Systems: Part 2-Design Live Loads on Box Culverts", *Department of Civil Engineering, University of Florida*, Project No. 4910 4504 857 12. 2002.
- [16] ASCE, "Standard Practice for Direct Design of Buried Precast Concrete Pipe Using Standard Installations (SIDD)", (ASCE 15-98), *American Society of Civil Engineers*, Reston, Virginia. 2000.
- [17] E. Winkler, "Die Lehre Von Elasticität Und Festigkeit". 1st Edn., *H. Dominicus*, Prague, 1867.
- [18] M. Hetenyi, "Beams on elastic foundation", *Waverly press*, Baltimore, 1946.
- [19] S. Lee, J. H. Ryu, I. S. Kim, "Landslide susceptibility analysis and its verification using likelihood ratio, logistic regression, and artificial neural network models: Case study of Youngin, Korea", *Landslides*, vol. 4, pp. 327-338. 2007.
- [20] S. Karimi, O. Kisi, J. Shiri, O. Makarynsky, "Neuro-fuzzy and neural network techniques for forecasting sea level in Darwin Harbor, Australia", *Computers and Geosciences*, vol. 52, pp. 50-59, 2013.
- [21] Y. Erzin, Y. Tuskan, "Prediction of standard penetration test (SPT) value in Izmir, Turkey using radial basis neural network", *Celal Bayar University Journal of Science*, vol.13, no.2, pp.433-439, 2017.
- [22] S. A. Yildizel, Y. Tuskan, G. Kaplan, "Prediction of skid resistance value of glass fiber-reinforced tiling materials", *Advances in Civil Engineering*, 2017.
- [23] B. Y. Dagli, Y. Tuskan, D. Uncu, "Artificial Neural Networks For Hydraulic Systems", *Research and Reviews In Engineering-Summer*, 2019, 85.

- [24] Y. Tuskan, B. Y. Dagli, D. Uncu, "The Use Of Artificial Neural Networks (Anns) In Geotechnics", Research and Reviews In Engineering–Summer, 2019, 225.
- [25] Y. Erzin, Y. Tuskan, "Prediction of Standard Penetration Test (SPT) Value in Izmir, Turkey using General Regression Neural Network", In International Conference on Agricultural, Civil and Environmental Engineering (ACEE-16) April 2016, pp. 18-19.
- [26] Y. Erzin, Y. Tuskan, "The use of neural networks for predicting the factor of safety of soil against liquefaction", Scientia Iranica, vol.26, no.5, pp. 2615-2623, 2019.
- [27] H. Sonmez, C. Gokceoglu, H. A. Nefeslioglu, A. Kayabasi, "Estimation of rock modulus: For intact rocks with an artificial neural network and for rock masses with a new empirical equation". International Journal of Rock Mechanics and Mining Sciences, vol. 43, no.2, pp.224-235, 2006.
- [28] N. Q. Hung, M. S. Babel, S. Weesakul, N. K. Tripathi, "An artificial neural network model for rainfall forecasting in Bangkok, Thailand", Hydrology and Earth System Sciences, vol. 13, no.8, pp.1413-1425, 2009.
- [29] E. Ebrahimi, M. Monjezi, M. R. Khalesi, D. J. Armaghani, "Prediction and optimization of back-break and rock fragmentation using an artificial neural network and a bee colony algorithm", Bulletin of Engineering Geology and the Environment, vol. 75, pp. 27-36, 2016.
- [30] T. K. Gupta, K. Raza, "Optimization of ANN architecture: a review on nature-inspired techniques". Machine learning in bio-signal analysis and diagnostic imaging, pp.159-182, 2019.
- [31] N. Singh, A. Singh, M. Tripathy, "Selection of hidden layer neurons and best training method for ffnn in application of long-term load forecasting". Journal of electrical engineering, vol.63, no.3, pp.153-161, 2012.
- [32] M. A. Shahin, H. R. Maier, M. B. Jaksa, "Data division for developing neural networks applied to geotechnical engineering". Journal of Computing in Civil Engineering, vol.18, no.2, pp.105-114, 2004.